Through-Bond Interactions in Silicon–Phosphorus and Silicon–Arsenic Compounds: A Facile Synthesis of Dodecamethyl-2,3,5,6,7,8-hexasila-1λ^3,4λ^3-diphosphabicyclo[2.2.2]octane, Its Arsenic Analogue, and Related Compounds

Uwe Winkler, Mathias Schieck, Hans Pritzkow, Matthias Driess,* Isabella Hyla-Kryspin, Holger Lange, and Rolf Gleiter*

Abstract: Dodecamethyl-2,3,5,6,7,8-hexasila-1λ^3,4λ^3-diphosphabicyclo[2.2.2]octane (**1**) and its arsenic analogue **2** are readily accessible in 69 and 73% yield, respectively, by the cyclocondensation reaction of 1,2-dichloro-1,1,2,2-tetramethyldisilane (**5**) with the lithium pnictides [LiEH$_2$(dme)] (E = P (**6**), As(**7**); dme = 1,2-dimethoxyethane). The reactions proceed via 1,4-diphosphaoctamethyltetrasilacyclohexane (**8**) and its arsenic analogue **9**, respectively, which were isolated and structurally characterized by X-ray crystallography. The molecular structures of **1** and **2**, which are isotypic, were also established by single-crystal X-ray analysis: they possess D_3 point symmetry with the expected Si–E bond lengths (E = P, As) but unusually long Si–Si bonds. The latter are 0.02–0.03 Å longer than those in **8** and **9**, mainly due to through-bond interactions (TB) between donating n orbitals of the E atoms and the σ* acceptor orbitals of the Si–Si bond. The first expanded analogues of **1**, namely, **12** and **14**, with hexamethyltrisilane and dodecamethylhexasilane chains bridging the two phosphorus atoms, were synthesized in a one-pot cyclocondensation reaction of the corresponding 1,3- and 1,6-dichlorooligosilanes **11** and **13**, respectively, with [LiPH$_2$(dme)] **6**. Ab initio calculations on the parent compounds **1a**, **12a**, and the second-row analogue 1,4-diazabicyclo[2.2.2]octane (**B**) were carried out in order to analyze the different coupling constants and magnitudes of intramolecular interactions (through-space/through-bond coupling). TS and TB coupling in **B** were found to be about two times stronger than in the congener **1a**, due to the compactness of the N_2C_6 skeleton and the greater extent of s,p hybridization at nitrogen. Evidence for TB interactions in **1** was obtained by photoelectron spectroscopy and by comparison of the two first vertical ionization potentials with calculated values for **1a**. The best agreement with experimental data was achieved when **1a** was calculated at the MP2 level. Compound **1a** preferentially adopts D_3 point symmetry; the higher-symmetry D_{3h} form possesses one imaginary frequency and is slightly less stable (0.46 kcal mol^{-1} at HF/6-31G*//HF/6-31G* and 1.58 kcal mol^{-1} at MP2/6-31G*//HF/6-31G* level), suggesting that this structure corresponds to a transition state on the potential energy surface. The structures corresponding to the global minimum of **B** and **12a** have D_{3h} and C_{3h} symmetry, respectively. At the HF/6-31G*//HF/6-31G* level the D_{3h} form of **12a** is 17.61 kcal mol^{-1} less stable than the C_{3h} minimum.

Keywords
ab initio calculations · arsenic · silicon · phosphorus · photoelectron spectroscopy

Introduction

The electronic structures of molecules and solids are dependent on their topology. In the case of unsaturated organic molecules and heterocycles it has been shown that certain topologies allow strong through-space/through-bond interactions.[1, 2] Studies on classical examples such as pyridazine (**A**)[3] and 1,4-diazabicyclo[2.2.2]octane (**B**)[4] revealed that the through-bond interaction between the nitrogen lone-pairs n_1 and n_2 is mediated by the σ framework. Detailed studies showed a large energy difference between the lone pairs (1.72 eV for **A** and 2.13 eV for **B**). Furthermore, the symmetrical linear combination of the lone-pairs $n_+ = 1/\sqrt{2(n_1+n_2)}$ is energetically disfavored in comparison to the antisymmetric linear combination $n_- = 1/\sqrt{2(n_1-n_2)}$. These interactions determine the electronic structure, stability, and reactivity of such compounds. The size of the gap between n_+ and n_- can be established by means of photoelectron spec-

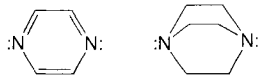

A **B**

[*] Prof. Dr. M. Driess,[+] Dr. U. Winkler, Dipl.-Chem. M. Schieck, Dr. H. Pritzkow
Anorganisch-chemisches Institut der Universität
Im Neuenheimer Feld 270, D-69120 Heidelberg (Germany)
Fax: Int. code +(6221)544-197
Dr. I. Hyla-Kryspin, H. Lange, Prof. Dr. R. Gleiter
Organisch-chemisches Institut der Universität
Im Neuenheimer Feld 270, D-69120 Heidelberg (Germany)
[+] New address: Fakultät für Chemie, Lehrstuhl für Anorganische Chemie I
Universitätsstraße 150, D-44801 Bochum (Germany)
Fax: Int. code +(234)709-4378
e-mail: driess@ibm.anch.ruhr-uni-bochum.de

0947-6539/97/0306-0874 $ 17.50+.50/0

troscopy and characterized by means of quantum chemical calculations within the one-electron model. It would be useful to be able to "design" the relay-like stabilization of electronically unusual compounds with appropriate topology (e.g., C_3 symmetric (radical) cations stabilized by through bond interactions), since this might allow the synthesis of compounds from heavy main-group elements with interesting electronic and optical properties. To date, the only known heavier analogues of **B** (containing the heavy main-group elements silicon, phosphorus,[5a] arsenic,[5b] antimony,[5b] and bismuth[5b]) expected to possess through-bond interactions are compounds **1**–**4**. However, the extent of such interactions has hitherto remained unexplored.

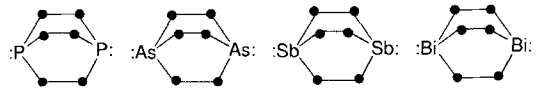

1: ● = $SiMe_2$ **2** **3** **4**
1a: ● = SiH_2

Here we report on an improved synthesis of **1** and **2** and on the first synthesis of structural analogues of **1**, bearing longer oligosilane chains $(SiMe_2)_n$ (n = 3 and 6) between the two phosphorus atoms. Furthermore, we present the PE spectroscopic characterization of **1**, ab initio calulations on the unsubstituted compounds $P(SiH_2)_6P$ (**1a**) and $P(SiH_2)_9P$ (**12a**), and the synthesis of the P,P′-diborane adduct of **1**. These results clearly prove the existence of relatively strong through-bond interactions in these heavier analogues of **B**.

Results and Discussion

The compounds **1** and **2** were first prepared by reaction of the 1,2-dichlorodisilane **5** with sodium/potassium phosphide and arsenide in relatively low yields (ca. 10 and 22%).[5a] We found that **1** and **2** are conveniently accessible in higher yields by reaction of **5** with $[LiEH_2(dme)]$ (E = P (**6**), E = As (**7**), Scheme 1). Formation of **1** and **2** occurred stepwise, via the respective diphospha- and diarsatetrasilacyclohexanes **8** and **9** as intermediates, after salt elimination. Lithiation of **8**/**9** by **6**/**7** and subsequent cyclocondensation with **5** gave rise to **1** and **2** in 69 and 73% yield, respectively, in the form of colorless crystals.

Compounds **8** and **9** were proven to be intermediates in the synthesis of **1** and **2**, respectively, since they were isolated in very low yields from the reaction mixtures by fractional crystallization. Compound **9** is thermolabile and decomposes in an argon atmosphere at 25 °C within 3 h to form an arsenic mirror, whereas **8** survives under such conditions. Their structures were established by X-ray structure analyses (Figure 1, Table 1).

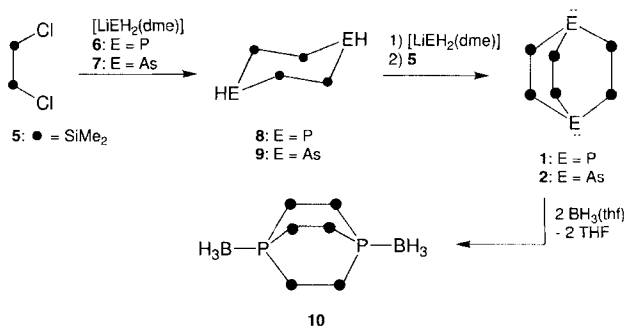

Scheme 1.

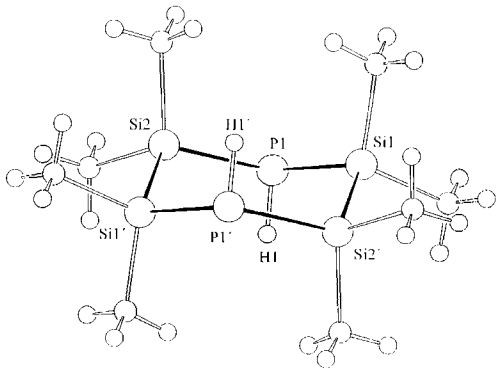

Figure 1. Solid-state structure of **8** (**8** is isotypic with **9**).

They crystallize isotypically in the trigonal space group $R\bar{3}$. The Si_4E_2 (E = P, As) chair is a little distorted and possesses approximately C_2 symmetry with a center of symmetry. The E–Si bond lengths are within the expected range for E–Si single bonds in acyclic silylphosphanes, silaphosphanes, and their arsenic analogues.[6] The Si–Si bond lengths of 2.340(1) Å in **8** and 2.332(2) Å in **9** are slightly different from those in dodecamethylcyclohexasilane $Me_{12}Si_6$.[7] The endocyclic angles in **9** are 115.31 and 115.64(7)° at silicon and 104.37(5)° at arsenic. These angles are only slightly different from those in **8** and related compounds, such as $PhP(SiMe_2)_4PPh$[8] (104.9(2)°), and in the cyclohexasilane $Me_{12}Si_6$[7] (111.9(5)°). The C1-Si1-

Table 1. Selected bond lengths [Å] and angles [°] for **1**, **2**, **8**, and **9**.

	1	**2**	**8**	**9**
E–Si	2.262(2)	2.363(1)	2.259(1), 2.261(1)	2.358(2), 2.358(2)
Si–Si′	2.363(2)	2.358(1)	2.340(1)	2.332(2)
Si–C	1.879(3), 1.884(2)	1.881(2), 1.881(2)	1.876(2), 1.885(2) 1.876(2), 1.880(5)	1.882(5), 1884(5) 1.883(5), 1884(5)
Si-E-Si′	101.50(4)	99.76(3)	105.70(3)	104.37(5)
E-Si-Si″	115.06(3)	116.22(2)	115.82(4), 115.78(4)	115.31(7)
C-Si-C	105.91(12)	106.24(10)	109.74(11), 109.59(10)	109.9(3), 109.7(3)
E-Si-C	108.08(9), 108.52(8)	107.89(7), 107.66(8)	108.04(7), 105.07(7) 107.87(8), 105.29(7)	108.5(2), 104.4(2) 107.8(2), 105.0(2)
Si′-Si-C	109.59(9), 109.28(10)	109.45(7), 108.92(8)	109.80(8), 108.20(8) 110.34(8), 107.75(8)	110.3(2), 108.3(2) 110.2(2), 108.2(2)

  0947-6539/97/0306-0875 $ 17.50+.50/0

Si2-C3 torsion angle in **9** is 172.1°, and the deviation from the ideal chair conformation is caused by the repulsive interaction of the axial methyl groups.

It has been concluded from IR and Raman spectroscopic investigations that **1** and **2** are of lower symmetry than the ideal D_{3h} structure.[5] We therefore determined the crystal structures of both compounds by X-ray diffraction analyses. The crystals are isotypic and possess C_{3i} point symmetry (Figure 2). Where-

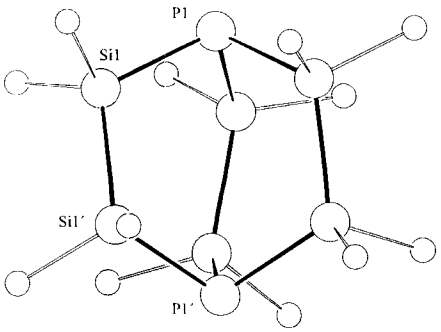

Figure 2. Molecular structure of **1** (**1** is isotypic with **2**).

as the Si–E bond lengths (E = P, As) show no unusual feature, the Si–Si bonds in both derivatives are 0.02–0.03 Å longer than in the less strained Si_4E_2 cyclic compounds **8** and **9**; the Si–C bond lengths in **1**, **2**, **8**, and **9** are identical. The main reason for the elongation of the Si–Si bonds in **1** and **2** is the through-bond interactions between donating n orbitals of the E atoms and the σ* acceptor orbitals of the Si–Si bonds. The molecular structure of the P,P'-diborane adduct **10**, formed in quantitative yield from **1** and [BH_3·(thf)] (2 equiv, Scheme 1), confirms the fact that electronic and not steric effects are mainly responsible for the longer Si–Si bonds. The structure analysis is not very accurate, owing to the poor crystal quality; therefore, a comparison of geometrical parameters with **1** is limited.[9] However, the Si–Si distance of 2.34(1) Å in **10** is shorter than that observed in **1** (2.363(2) Å), despite the greater steric congestion in the former.

Quantum Chemical Calculations and Photoelectron (PE) Spectroscopic Investigations: One of the aims of this report is to discuss the characteristic differences in the electronic structures of the isostructural homologues **1a** and **B**. Therefore we carried out ab initio calculations on these compounds, in order to analyze the different contributions (coupling) and magnitudes of intramolecular interactions (through-space (TS) and through-bond coupling (TB)). In addition, we compare the PE spectra of **1** and **B** as well as the calculated TS/TB couplings of **1a** with those of **12a**.

Molecular Geometries: Computational details are described in the Experimental Section. Results of the HF/6-31G*-optimized geometrical parameters of **1a**, **B**, and **12a** are collected in Table 2.

The agreement between calculated and experimental bond lengths and angles is very good. In the case of **1a** the calculations predict that the D_3 structure represents a global minimum on the potential energy surface, that is, no imaginary frequency

Table 2. Optimized structural parameters of **B**, **1a**, and **12a** (bond lengths in Å and angles in °; i = number of imaginary frequencies).

	Compound **B**			Compound **1a**			Compound **12a**	
	D_{3h}	Exp. [a]		D_{3h}	D_3	Exp. [b]	D_{3h}	C_{3h}
N–C	1.459	1.477	P–Si	2.268	2.270	2.262	2.244	2.261
C–C	1.555	1.590	Si–Si	2.375	2.371	2.363	2.371	2.363
C-N-C	109.1	108.1	Si-P-Si	103.0	102.1	101.5	115.10	109.4
N-C-C	109.8	110.5	P-Si-Si	115.4	114.2	115.1	128.61	120.3
N-C-C-N	0.0		P-Si-Si-P	0.0	24.1	22.1		
			P-Si-Si-Si				0.0	76.2
			Si-Si -Si					120.0
i	0			1	0		3	0

[a] Ref. [14]. [b] X-ray data of **1**, this work.

is observed. The C_3 structure of **1a** converges to the D_3 structure. The vibrational analysis for the D_{3h} isomer reveals one imaginary a_1'' mode at 42 cm^{-1}, suggesting that this structure corresponds to a transition state on the potential energy surface. An examination of the normal coordinates corresponding to this a_1'' mode suggests a distortion to the C_3 structure. However, the twisting of the $P(SiH_2)_3$ moieties in **1a** is not an energy-demanding process. At the HF/6-31G*//HF/6-31G* and MP2/6-31G*//HF/6-31G* levels, **1a** (D_{3h}) is, respectively, 0.46 and 1.58 kcal mol^{-1} less stable than **1a** (D_3). In contrast, during geometry optimizations both the D_3 and C_3 structures of **B** converge to D_{3h}, whose frequencies are all real. Remarkably, twisting of the $N(CH_2)_3$ units in **B** does not occur, due to the large strain energy of the D_{3h} form. In the case of **12a** the HF/6-31G*//HF/6-31G* calculations predict that the C_{3h} structure represents a global minimum on the potential energy surface (i = 0). During geometry optimizations the C_3 isomer converges to C_{3h}, and the D_{3h} structure with three imaginary frequencies does not correspond to a stationary point on the potential energy surface. At the HF/6-31G*//HF/6-31G* level, the D_{3h} structure of **12a** is 17.61 kcal mol^{-1} less stable than the C_{3h} minimum.

PE Spectrum of 1: The PE spectrum of **1** is shown in Figure 3. The first band with maximum at 6.9 eV is well separated from an overlapping broad band region with measurable maxima at 8.0, 8.6, 9.0, 9.5, and 10.5 eV (Figure 3). In order to assign the bands and to understand the TS/TB coupling, we first proceed empirically by comparing the bands of **1** with those of **B**, whose assignment is unequivocal.[2] The lower-energy part of the PE spectrum of **B** exhibits two well-resolved bands with maxima

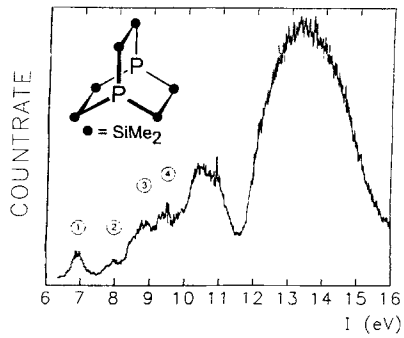

Figure 3. He(I) PE spectrum of **1**.

0947-6539/97/0306-0876 $ 17.50+.50/0 Chem. Eur. J. 1997, 3, No. 6

at 7.52 and 9.65 eV.[2] They are associated with ionization processes from the bonding n_+ (HOMO) and the antibonding n_- (HOMO − 1) combinations of the nitrogen lone-pair orbitals. The splitting between these bands ΔI_n (2.13 eV) provides an experimental measure for the TS and TB coupling. If we assume the same assignment as for **B** for the two first bands, the TS/TB coupling is then predicted to be about two times weaker (1.1 eV, Figure 4). In order to verify our empirical assignment we carried out an ab initio analysis of the TS and TB interactions for the model compound **1a** and for **B**, as discussed in the next section.

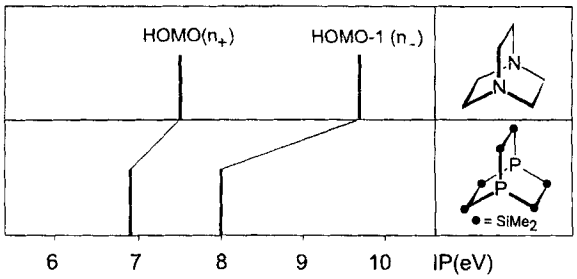

Figure 4. Correlation between the first ionization energies of **B** and **1**.

TS and TB interaction in ***1a****,* ***B****, and* ***12a***: In Table 3 we compare the two first ionization energies of **1** and **B** with the values calculated by assuming the validity of Koopmans's theorem ($I_v = -\varepsilon_i$)[10] as well as by using the ΔSCF (HF/6-31G*//HF/6-31G*) and the ΔMP2 (MP2/6-31G*//HF/6-31G*) methods. For both molecules the canonical orbital sequence locates n_+ above of n_-, and Koopmans's defects do not change this sequence. For **12a** the calculations predict the normal orbital sequence, that is, the out-of-phase combination (n_-) is located above the in-phase (n_+) combination. The calculated absolute values for the two first ionization potentials of **B** are reproduced accurately at the ΔSCF level; Koopmans's theorem overestimates and ΔMP2 underestimates the experimental values. In the case of **1a** the best agreement with experimental results is achieved at the MP2 level, that is, both relaxation and correlation effects must be included in the calculation procedure. We note, however, that in accord with the empirical assignment given in Figure 4, the calculated splitting ΔI_n of **1a** is about two times less than for **B**, independently of the level at which the calculations are performed (Table 3).

Table 3. The two first ionization energies of **B**, **1a**, and **12a** calculated by assuming the validity of Koopmans's theorem ($-\varepsilon_j$) and by using the ΔSCF and ΔMP2 aproach. All values are given in eV.

	Band	$-\varepsilon_j$	ΔSCF	ΔMP2	I_{vij} [a]	Assignment
B (D_{3h})	1	8.39	7.33	6.51	7.52	$^2A_1'$: HOMO(n_+)
	2	11.29	9.60	8.84	9.65	$^2A_2''$: HOMO − 1(n_-)
	ΔI_n [b]	2.90	2.27	2.33	2.13	
1a (D_3)	1	8.29	7.76	7.24	6.90	$^2A_1$: HOMO(n_+)
	2	9.69	8.92	8.49	8.00	$^2A_2$: HOMO − 1(n_-)
	ΔI_n [b]	1.40	1.16	1.25	1.10	
12a (C_{3h})	1	8.31	7.80	7.00		$^2A''$: HOMO(n_-)
	2	8.89	8.28	7.34		$^2A'$: HOMO − 1(n_+)
	ΔI_n [b]	0.58	0.48	0.34		

[a] Experimental value for **B** (ref. [4]) and **1** (this work). [b] Splitting between bands 1 and 2.

In principle, the final energetic splitting ΔI_n may be a result of TB and/or TS interactions. Table 3 provides little insight into the factors responsible for the magnitude of the two types of interactions. In order to obtain a deeper insight into the nature of these interactions, the canonical molecular orbitals (CMOs) of the ground state HF wave function of **1a**, **B**, and **12a** were transformed into localized orbitals, for which we used the natural bond orbitals (NBOs) of Weinhold et al.[11] For the quantitative treatment we applied the procedure of Imamura et al.[12] The corresponding NBO interaction diagrams of **1a** and **12a** are shown in Figures 5 and 6. The results obtained for **B** are discussed in the text.

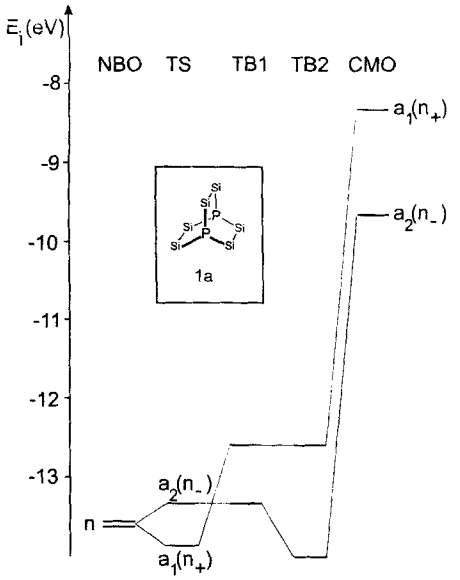

Figure 5. TS/TB interaction diagram of **1a**; NBO: energy of the degenerate, noninteracting n NBOs; TS: energy after the TS interaction; TB1: energy after the addition of three σ(Si–Si) NBOs; TB2: energy after the addition of three σ*(Si–Si) NBOs; CMO: energy of CMOs.

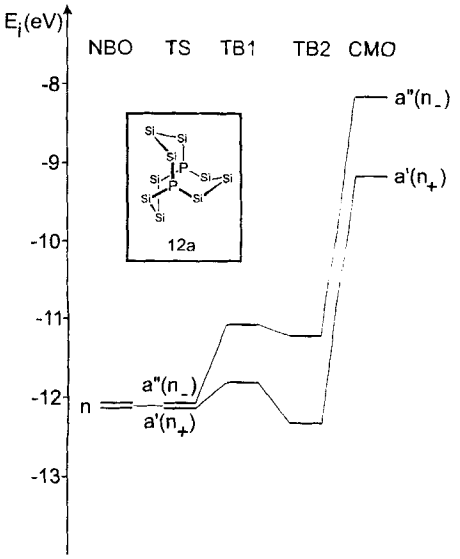

Figure 6. TS/TB interaction diagram of **12a**. NBO: energy of the degenerate, noninteracting n NBOs; TS: energy after the TS interaction; TB1: energy after the addition of six σ(Si–Si) NBOs; TB2: energy after the addition of six σ*(Si–Si) NBOs; CMO: energy of CMOs.

The basis energies of the degenerate, noninteracting lone-pair n NBOs are displayed on the left-hand side of Figures 5 and 6, respectively. The diagonalization of the 2×2 NBO Fock matrix involving n NBOs gives the energies of the symmetry-adapted precanonical molecular orbitals (PCMOs) n_+ and n_- in the absence of TB coupling. The calculated TS energy gap between PCMOs $a'_1(n_+)$ and $a''_2(n_-)$ of **B** is 1.34 eV. As shown in Figure 5 and 6, the PCMOs $a_1(n_+)$ and $a_2(n_-)$ of **1a** resulting from TS coupling are separated by only 0.49 eV. Neither for **1a** nor for **B** do these splittings reproduce the final (i.e., canonical and experimental) results. Thus, a direct orbital interaction, that is, TS homoconjugation, cannot be the only factor responsible for the energetic splitting ΔI_n found in the PE spectra of **1** and **B**. The TS interaction in **1a** is weaker than in **B**, owing to the large P–P distance (d_{P-P} = 4.321 Å (**1a**) vs. d_{N-N} = 2.545 Å (**B**)) and the greater s character of the n NBOs (43% (**1a**) vs. 17% (**B**)). Clearly, the latter is a result of the reluctance of heavier (3rd period and above) main-group elements to undergo s,p hybridization.[13] In order to investigate the TB interactions we built up the NBO matrices by successively adding in groups the sets of σ and σ* NBOs, and at each step we diagonalized the appropriate sub NBO Fock matrix. Since the NBO sets provide basis functions for the symmetry-adapted PCMOs, for each diagonalization step it is important to add a complete set of the particular NBOs. In the last step we diagonalized the full NBO Fock matrix. This gives the CMOs in the NBO basis. The most important TB splittings of **1a** and **12a** are shown in Figures 5 and 6 and those of **B** are discussed in the text. While PCMOs n_+ and n_- of **B**, **1a**, and **12a** transform according to the one-dimensional representation, it is clear that PCMOs belonging to the degenerate representations will not contribute to the TB couplings. In the case of **B** and **1a** only the n_+ combination matches with one PCMO, namely, σ(C–C/Si–Si). This TB1 interaction destabilizes the PCMO $a_1(n_+)$ of **1a** and $a'_1(n_+)$ of **B** by 1.2 and 1.63 eV, respectively. In the TB1 interaction the energy of PCMO n_- remains unchanged, and this results in the inverted PCMO sequence, with n_+ above n_-. Subsequently, admixture of PCMOs σ*(C–C/Si–Si) (a_2 of **1a** and a''_2 of **B**), denoted as TB2 interaction, stabilizes the PCMO n_- by 0.63 eV (**1a**) and 1.31 eV (**B**). Again, both TB interactions are stronger in **B** than in **1a**. The donor–acceptor TB2 interaction leads to electron density transfer from n_- NBOs to the σ*(C–C/Si–Si) NBOs. According to the NBO population analysis, the calculated occupancy of the n NBOs is significantly lower than 2.00 (1.924 (**1a**), 1.923 (**B**)) and those of σ*(Si–Si) and σ*(C–C) are 0.043 and 0.033, respectively (see Table 4). These results explain the experimentally observed elongated Si–Si/C–C bonds in **1** and **B** (2.363 Å (**1**), 1.590 Å (**B**)[14]). As shown in Figure 5, after TS + TB1 + TB2 interactions the PCMOs n_+ and n_- of **1a** are already separated by 1.34 eV, which approximately corresponds to the final (i.e., canonical and experimental) results of **1** (see Table 3). For **B**, however, the calculated splitting at this step is 1.60 eV, and interactions of longer range seem to be important to reproduce the canonical splitting.

Table 4. Results of NBO population analysis for **B**, **1a**, and **12a** (OCC = occupation numbers).

NBO	OCC(**B**)	NBO	OCC(**1a**)	OCC(**12a**)
n	1.923	n	1.924	1.900
σ(CC)	1.995	σ(SiSi)	1.973	1.974
σ(NC)	1.984	σ(PSi)	1.973	1.978
σ(CH)	1.987	σ(SiH)	1.988	1.986
σ*(CC)	0.033	σ*(SiSi)	0.043	0.032
σ*(NC)	0.015	σ*(PSi)	0.018	0.020
σ*(CH)	0.011	σ*(SiH)	0.020	0.012

Although the PE spectroscopic investigation of **12** was not possible, a short comparison of the TS/TB couplings in **1a** and **12a** may be instructive. With respect to **1a**, the basis energy of the noninteracting lone-pair NBOs of **12a** is shifted to higher energy, due to the difference in s character of the n NBOs (43% (**1a**) vs. 34% (**12a**)). In **12a** the large P–P distance of 5.601 Å prevents an efficient overlap between n NBOs, and consequently the TS coupling is practically absent. The calculated TS splitting is only 0.01 eV. In contrast to **1a** both PCMOs n_+ and n_- of **12a** match with PCMOs constructed from Si–Si σ and σ* NBOs. Thus, PCMOs $a'(n_+)$ and $a''(n_-)$ will both be affected by the TB1 and TB2 interactions. The TB1 interaction destabilizes the PCMOs n_+ and n_- by 0.26 and 1.01 eV, respectively. The normal PCMO sequence with n_- above n_+ remains unchanged. The TB2 interaction does not change this sequence; the PCMOs $a'(n_+)$ and $a''(n_-)$ are stabilized by 0.45 and 0.17 eV, respectively (Figure 6). The TS and TB interactions in **1a** are stronger than in **12a** and consequently the canonical splitting for **12a** (0.58 eV) is more than two times smaller than for **1a** (1.40 eV) (Table 3). It is interesting to note that the splitting between the two first bands found in the PE spectrum of the analogous molecule 1,5-diphosphabicyclo[3.3.3]undecane is 0.56 eV.[15]

Syntheses of the Expanded Analogues 12 and 14: The strategy used for the synthesis of **1** can be surprisingly easily adapted to expanded polysilane systems. Thus, reaction of **6** with the dichlorooligosilanes **11** and **13** gave rise to the respective heterobicycles **12** and **14**, which were isolated in 24 and 16% yields, respectively (Scheme 2). The composition of both products was

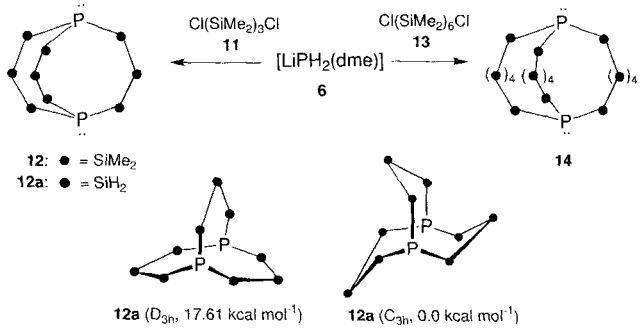

Scheme 2.

determined by mass spectrometry, and the structures were unambiguously established from the characteristic simple appearance of the ^1H and ^{31}P NMR spectra. The singlets in the ^{31}P NMR spectra of **12** and **14** are shifted slightly downfield compared to the corresponding signal in the spectrum of **1**. The methyl protons of the α-$SiMe_2$ groups in **12** give a doublet at $\delta = 0.37$ ($^3J(H,P) = 5$ Hz), and the protons of the β-$SiMe_2$ groups give a singlet at $\delta = 0.14$. The ^1H NMR spectrum of **14** is almost identical to that of **12**, except that the methyl protons of the α-$SiMe_2$ groups appear as a singlet.

0947-6539/97/0306-0878 $ 17.50+.50/0 Chem. Eur. J. 1997, 3, No. 6

Owing to the relatively high molecular weight of **12** and **14**, a PE spectroscopic investigation of these compounds has so far not been possible. Thus, the extent TB interactions in **12** and **14**, compared to **1**, has not yet been experimentally determined.

Conclusion

We have shown that **1** and its arsenic analogue **2** are readily prepared in high yields by reaction of the 1,2-dichlorodisilane **5** with lithium phosphide **6** and arsenide **7**, respectively. This method can be adapted for the synthesis of the novel expanded polysilane homologues **12** and **14**. The PE spectroscopic study of **1** and ab initio calculations on the parent compound **1a** give evidence for relatively strong TB interactions in this system. The ab initio calculations on **1a** and **B** give, for the first time, qualitative and quantitative insight into the magnitude of TS/TB coupling. The magnitude of TB interactions in the second-row analogue **B** is approximately twice that in **1**, because of the compactness of the N_2C_6 skeleton and the different extent of s,p hybridization at nitrogen. The ab initio calculations reveal that through-space interactions are not present in **12a**. The through-bond interactions of **12a** are weaker than those of **1a**. Further studies are necessary to gain insight into the influence of the length of the silicon chain and of its branching on the strength of TB interactions in other analogues of **1**.

Experimental Section

All experiments were performed under anaerobic conditions using Schlenk tube techniques. The starting materials **5**,[15] **6** and **7**,[16] **11**,[17] and **13**[18] were prepared as described in the literature. ^{1}H, ^{31}P, and ^{11}B NMR spectra were recorded on a Jeol-FX90Q (^{31}P: 36.6, ^{11}B: 28.7 MHz). Chemical shifts are given in ppm relative to respective standards. External standards for ^{31}P NMR: 85% aq. H_3PO_4; ^{11}B NMR: $F_3B{-}OEt_2$; ^{1}H NMR: $SiMe_4$. Mass spectra (MS) were obtained on a Finnigan MAT8230. The He(I)-PE spectrum of **1** was recorded on a PS18 spectrometer (Perkin-Elmer). The measurement temperature was 160 °C (calibration: Ar and Xe).

Dodecamethyl-2,3,5,6,7,8-hexasila-1λ^3,4λ^3-diphosphabicyclo[2.2.2]octane (1), 1,4-Diphospha-1,4-dihydro-2,2,3,3,5,5,6,6-octamethyl-2,3,5,6-tetrasila-cyclohexane (8), and Their Arsenic Analogues (2) and (9):

1: A solution of **6** (13.2 g, 0.1 mol) in THF (160 mL) at −50 °C was allowed to react with **5** (9.6 g, 0.05 mol) for 2 h. The mixture was then allowed to warm up to room temperature and stirred for 2 h. After removal of all volatile components at 25 °C in vacuo (10^{-2} Torr), the residue was taken up in hexane (120 mL), and the salt was filtered off through a GIV frit. The clear solution was concentrated to give colorless crystals of **1** at 25 °C. Yield: 4.7 g (11.5 mmol), 69%.

2: A similar procedure was used to that for the synthesis of **1**, starting from **7** (15.2 g, 87 mmol) in 80 mL of THF and **5** (8.2 g, 44 mmol). Fractional crystallization at −20 °C afforded **2** in the form of colorless crystals. Yield: 5.3 g (10.7 mmol), 73%.

The analytical data of **1** and **2** are identical with those reported in refs [4, 5].

8 and **9**: These compounds were isolated by fractional crystallization from the reaction mixtures for the synthesis of **1** and **2** as described above. They were isolated in the form of air- and water-sensitive colorless crystals. **9** is thermolabile and slowly decomposes above −20 °C.

8: Yield: 1.27 g (4.26 mmol), 8.4%; ^{1}H NMR ([D^8]THF): $\delta = 0.30$ (d, 24H, $SiMe_2$, ^3J(H,P) = 5.6 Hz), 1.45 (d, 2H, PH, ^1J(H,P) = 186 Hz); ^{31}P NMR ([D^8]THF): $\delta = -253.7$ (d, ^1J(P,H) = 186 Hz). MS (EI) *m/z* (%): 296 (54) [M^+], 238 (17) [$(M - SiMe_2)^+$], 178 (3) [$P_2(SiMe_2)_2^+$], 73 (100) [$SiMe_3^+$]; high-resolution MS for $C_8H_{26}P_2Si_4$: calcd. 296.5940 found 296.5826.

9: Yield: 422 mg (1.1 mmol), 5%; ^{1}H NMR ([D^8]THF): $\delta = 0.32$ (s, 24H, $SiMe_2$), 1.25 (s, 2H, AsH). MS (EI) *m/z* (%): 384 (22) [M^+], 326 (11) [$(M - SiMe_2)^+$], 266 (3) [$As_2(SiMe_2)_2^+$], 73 (100) [$SiMe_3^+$]; high-resolution MS for $C_8H_{26}As_2Si_4$: calcd. 384.4898 found 384.4865.

Diborane Adduct (10): A solution of **1** (0.73 g, 1.8 mmol) in 30 mL of THF was treated with a 1 M solution of the borane–THF complex (5.4 mL) at −60 °C. The solution was warmed up to room temperature and stirred for 12 h. All volatile components were removed in vacuo (25 °C, 10^{-2} Torr) and the residue was recrystallized from THF to give a colorless solid (m.p. 220 °C (decomp.)); quantitative yield, 0.76 g (1.8 mmol). ^{1}H NMR (C_6D_6): $\delta = 0.38$ (d, 36H, ^3J(H,P) = 6.3 Hz, $SiMe_2$), 3.52 (brq, 6H, BH); $^{11}B\{^1H\}$ NMR (C_6D_6): $\delta = -35.0$ (s); ^{31}P NMR ([D^8] THF, 25 °C): −189.6 (s). MS (EI) *m/z* (%): 438 (1) [M^+], 410 (13) [$(M - 2BH_3)^+$], 73 (100) [$SiMe_3^+$]; high-resolution MS for $C_{12}H_{42}B_2P_2Si_6$: calcd. 438.1560, found 438.1551.

Octadecamethyl-2,3,4,6,7,8,9,10,11-nonasila-1λ^3,5λ^3-diphosphabicyclo[3.3.3]undecane (12): A similar procedure was used to that for the synthesis of **1**, starting from **6** (4.41 g, 33.6 mmol) in THF (50 mL) and **13** (4.10 g, 16.8 mmol). The colorless product was crystallized in hexane (10 mL) at −20 °C. Yield: 770 mg (1.3 mmol), 24%; m.p. 150 °C (decomp.). ^{1}H NMR (C_6D_6): $\delta = 0.14$ (s, 18H, β-$SiMe_2$), 0.37 (d, 36H, ^3J(H,P) = 5 Hz, α-$SiMe_2$); ^{31}P NMR (C_6D_6): $\delta = -243.2$ (s). MS (EI) *m/z* (%): 584 (2) [M^+], 410 (12) [$(P_2(SiMe_2)_6)^+$], 73 (100) [$SiMe_3^+$]; high-resolution MS for $C_{18}H_{54}P_2Si_9$: calcd. 584.1607, found 584.1598.

Tetrapentacontamethyl-2,3,4,5,6,7,9,10,11,12,13,14,15,16,17,18,19,20-octadecasila-1λ^3,8λ^3-diphosphabicyclo[6.6.6]eicosane (14): A similar procedure was used to that for the synthesis of **1**, starting from **6** (0.95 g, 7.3 mmol) in THF (15 mL) and **13** (1.52 g, 3.65 mmol). The colorless product was crystallized from hexane (5 mL) at −20 °C and melts at room temperature. Yield: 220 mg (0.2 mmol), 16.2%. ^{1}H NMR (C_6D_6): $\delta = 0.17$ (s, 72H, Si-$SiMe_2$-Si), 0.39 (s, 36H, α-$SiMe_2$); ^{31}P NMR (C_6D_6): $\delta = -234.3$ (s). MS (EI) *m/z* (%): 1106 (5) [M^+], 410 (1) [$(SiMe_2)_6^+$], 73 (100) [$SiMe_3^+$]; high-resolution MS for $C_{36}H_{108}P_2Si_{18}$: calcd. 1106.3740, found 1106.3738.

Computational Details: All calculations were carried out with a 6-31G* basis using the Gaussian 94 system of programs.[18] The structures of **1a**, **B**, and **12a** were gradient-optimized at the Hartree-Fock (HF) level. In order to check the stationarity, the equilibrium geometries of the isomers were used for analytical calculations of the Hessian matrices. The PE spectrum was calculated according to Koopmans's theorem[10] and by employing the ΔSCF approach at the HF/6-31G*//HF/6-31G* and MP2/6-31G*//HF/6-31G* levels. In order to quantify the through-bond (TB) interactions, the canonical molecular orbitals (CMOs) of the HF wave functions were transformed into a set of natural bond orbitals (NBOs) according to the Weinhold localization procedure.[11] The variation in the lone-pair energies due to through-space (TS)/TB interactions was calculated by diagonalization of the particular blocks of the NBO Fock matrix containing selected subsets of interacting orbitals. A detailed description of the NBO pathway approach as applied to the analysis of TS/TB interactions can be found in the literature.[12]

X-Ray Structural Analyses: Experimental details on the X-ray crystal structure determinations of **1**, **2**, **8**, and **9** are listed in Table 5. Intensity data were collected on a Siemens-Stoe AED2 ($Mo_{K\alpha}$ radiation, ω scan), for **1** at room temperature, for **2**, **8**, and **9** at −70 °C. The structures were solved by direct methods (SHELXS86) and refined by full-matrix least-squares methods based on F^2 using all measured reflections (SHELXL93) with anisotropic temperature factors for all non-hydrogen atoms. Hydrogen atoms in **1**, **2**, and **8** were located in difference Fourier maps and refined isotropically; in **9** they were inserted in calculated positions, but not refined.

Crystallographic data (excluding structure factors) for the structures reported in this paper have been deposited with the Cambridge Crystallographic Data Centre as supplementary publication no. CCDC-100143. Copies of the data can be obtained free of charge on application to The Director, CCDC, 12 Union Road, Cambridge CB21EZ, UK (Fax: Int. code +(1223)336-033; e-mail: deposit@chemcrys.cam.ac.uk).

Acknowledgements: We thank the Deutsche Forschungsgemeinschaft (Sonderforschungsbereich 247) and the Fonds der Chemischen Industrie for financial support.

Received: October 10, 1996 [F489]

Table 5. Crystal data and structure refinement for compounds **1**, **2**, **8**, and **9**.

	1	**2**	**8**	**9**
formula	$C_{12}H_{36}P_2Si_6$	$C_{12}H_{36}As_2Si_6$	$C_6H_{26}P_2Si_4$	$C_8H_{26}As_2Si_4$
formula weight	410.89	498.79	296.59	384.49
T [K]	293(2)	203(2)	203(2)	203(2)
crystal system	trigonal	trigonal	monoclinic	monoclinic
space group	$R\bar{3}$	$R\bar{3}$	$P2_1/n$	$P2_1/n$
a [Å]	9.711(8)	9.767(5)	6.971(4)	7.036(4)
b [Å]	9.711(8)	9.767(5)	12.440(6)	12.580(6)
c [Å]	44.29(3)	43.99(2)	10.236(5)	10.297(5)
α [°]	90	90	90	90
β [°]	90	90	92.22(4)	92.71(3)
γ [°]	120	120	90	90
V [Å^3]	3617(5)	3634(3)	887.0(8)	910.4(8)
Z	6	6	2	2
ρ_{calcd} [g cm^{-3}]	1.132	1.368	1.110	1.395
$F(000)$	1332	1548	320	388
crystal size [mm]	0.7 × 0.6 × 0.35	0.5 × 0.3 × 0.3	0.2 × 0.4 × 0.6	0.2 × 0.4 × 0.6
θ_{max} [°]	30.0	33.0	26.0	27.0
hkl range	−11/11, 0/13, 0/62	−12/12, 0/14,0/67	−8/8, 0/15, 0/12	−8/8, 0/16, 0/13
reflns collected	2171	2820	1744	1984
reflns independent	1186 [R_{int} = 0.030]	1527 [R_{int} = 0.028]	1744	1984
abs. coeff. [cm^{-1}]	4.71	30.50	4.89	39.1
transmission	0.938–0.999	0.750- 0.822	0.866–0.999	0.482 0.999
parameters	56	56	116	69
GOF on F^2	1.032	1.080	1.051	1.049
$R1$ [$I>2\sigma(I)$]	0.031	0.024	0.026	0.050
$wR2$ (all data)	0.080	0.055	0.067	0.121
resid. elec. dens. [e Å^{-3}]	0.22/−0.16	0.28/−0.32	0.27/−0.29	2.32/−1.68

[1] R. Hoffmann, A. Imamura, W. J. Hehre, *J. Am. Chem. Soc.* **1968**, *90*, 1499.

[2] Reviews: R. Hoffmann, *Acc. Chem. Res.* **1971**, *Vol. 4*, 1; R. Gleiter, *Angew. Chem.* **1974**, *86*, 770; *Angew. Chem. Int. Ed. Engl.* **1974**, 13, 696; R. Gleiter, W. Schäfer, *Acc. Chem. Res.* **1990**, *23*, 369; M. N. Paddon-Row, *ibid.* **1982**, *15*, 245; M. Eckert-Maksic' in *Theoretical Models of Chemical Bonding* (Ed.: Z. B. Maksic'), Springer, Heidelberg, Germany, **1991**, p. 153.

[3] R. Gleiter, E. Heilbronner, V. Hornung, *Helv. Chim. Acta* **1972**, *55*, 255.

[4] E. Heilbronner, K. A. Muszkat, *J. Am. Chem. Soc.* **1970**, *92*, 3818

[5] a) K. Hassler. *J. Organomet. Chem.* **1983**, *246*, C31; b) K. Hassler, S. Seidl, *ibid.* **1988**, *347*, 27.

[6] G. Becker, G. Gutekunst, C. Witthauer, *Z. Anorg. Allg. Chem.* **1982**, *486*, 90; W. Hönle, H. G. von Schnering, *Z. Naturforsch.* **1980**, *35B*, 789; M. Driess, R. Janoschek, H. Pritzkow, *Angew. Chem.* **1992**, *104*, 449; *Angew. Chem. Int. Ed. Engl.* **1992**, *31*, 460.

[7] H. H. Carell, J. Donohue, *Acta Crystallogr.* **1972**, *28B*, 1566.

[8] A. W. Cordes. P. F. Schubert, R. T. Oakley, *Can. J. Chem.* **1979**, *57*, 174.

[9] Preliminary crystallographic data for **10**: Monoclinic $P2_1/a$, a = 13.720(7), b = 13.848(7), c = 13.279(7) Å, β = 93.27(4)°, V = 2708 Å^3, Z = 4.

[10] T. Koopmans, *Physica* **1934**, *1*, 104.

[11] A. E. Reed, R. B. Weinstock, F. Weinhold, *J. Chem. Phys.* **1985**, *83*, 735; A. E. Reed, F. Weinhold, *ibid.* **1983**, *78*, 4066.

[12] A. Imamura, M. Ohsaku, *Tetrahedron* **1981**, *37*, 2191. Use of NBOs to analyze the TS/TB interaction: M. N. Paddon-Row, K. D. Jordan, *J. Chem. Soc. Chem. Commun.* **1988**, 1508; M. N. Paddon-Row, S. S. Wong, K. D. Jordan, *J. Am. Chem. Soc.* **1990**, *112*, 1710; *ibid. J. Chem. Soc. Perkin Trans 2* **1990**, 414; C. A. Naleways, L. A. Curtiss, J. R. Miller, *J. Phys. Chem.* **1991**, *95*, 8434; C. Liang, M. Newton, *ibid.* **1992**, *96*, 2855; M. N. Paddon-Row, K. D. Jordan, *J. Am. Chem. Soc.* **1993**, *115*, 2952; R. Gleiter, H. Lange, O. Borzyk, *ibid.* **1996**, *118*, 4889; see also E. Heilbronner, A. Schmelzer, *Helv. Chim. Acta* **1975**, *58*, 936.

[13] W. Kutzelnigg, *Angew. Chem.* **1984**, *96*, 262; *Angew. Chem. Int. Ed. Engl.* **1984**, *23*, 272; R. Janoschek, *Chem. Unserer Zeit* **1988**, *21*, 128; W. W. Schoeller in *Multiple Bonds and Low Coordination in Phosphorus Chemistry* (Eds.: M. Regitz, O. J. Scherer), Thieme, Stuttgart, **1990**, p. 8.

[14] T. Wada, E. Kishiola, Y. Tomiie, H. Suga, S. Seki, I. Nitta, *Bull. Chem. Soc. Jpn.* **1960**, *33*, 1317.

[15] R. W. Alder, D. D. Ellis, C. Ganter, C. J. Harris, J. K. Hogg, A. Martin, A. G. Orpen, P. N. Taylor, R. Gleiter, H. Lange, unpublished results.

[16] H. Sakurai, K. Tominaga, T. Watanabe, M. Kumada, *Tetrahedron Lett.* **1966**, *45*, 5493.

[17] H. Schäfer, G. Fritz, W. Hölderich, *Z. Anorg. Allg. Chem.* **1977**, *428*, 222; G. Becker, M. Schmidt, M. Westerhausen, *ibid.* **1992**, *607*, 101.

[18] G. Fritz, B. Grunert, *Z. Anorg. Allg. Chem.* **1981**, *473*, 59, and ref. [15].

[19] H. Gilman, R. A. Tomasi, *J. Org. Chem.* **1963**, *28*, 1851; S. M. Chen, A. Katti, T. A. Blinka, R. West, *Synth.* **1985**, *684*, 684; H. Gilman, S. Inoue, *J. Org. Chem.* **1964**, *29*, 3418.

[20] GAUSSIAN94, Revision B. 3., M. J. Frisch, G. W. Trucks, H. B. Schlegel, P. M. W. Gill, B. G. Johnson, M. A. Robb, J. R. Cheeseman, T. Keith, G. A. Petersson, J. A. Montgomery, K. Raghavachari, M. A. Al-Laham, V. G. Zakrzewski, J. V. Oritz, J. B. Foresman, C. Y. Peng, P. Y. Ayala, W. Chen, M. W. Wong, J. L. Andres, E. S. Replogle, R. Gomperts, R. L. Martin, D. J. Fox, J. S. Binkley, D. J. Defrees, J. Baker, J. P. Stewart, M. Head-Gordon, C. Gonzalez, J. A. Pople, Gaussian, Pittsburgh PA, **1995**.

 0947-6539/97/0306-0880 $ 17.50+.50/0